

Bose-Einstein condensates in ‘giant’ toroidal magnetic traps

A. S. Arnold and E. Riis

*Department of Physics and Applied Physics, University of Strathclyde, 107 Rottenrow, Glasgow G4 0NG, UK**

Abstract. The experimental realisation of gaseous Bose-Einstein condensation (BEC) in 1995 [1] sparked considerable interest in this intriguing quantum fluid [2]. Here we report on progress towards the development of an ^{87}Rb BEC experiment in a large (≈ 10 cm diameter) toroidal storage ring. A BEC will be formed at a localised region within the toroidal magnetic trap, from whence it can be launched around the torus. The benefits of the system are many-fold, as it should readily enable detailed investigations of persistent currents, Josephson effects, phase fluctuations and high-precision Sagnac or gravitational interferometry.

The idea [3] of neutral atomic and molecular storage rings has only very recently been realised experimentally: fast polar molecules were stored in a 25 cm diameter electrostatic hexapole ring [4], and laser-cooled neutral ^{87}Rb atoms have been confined in a 2 cm diameter two-wire toroidal magnetic guide with an ≈ 1 s lifetime [5]. We believe our ‘BEC-friendly’ approach to toroidal neutral atom storage will have additional advantages, ensuring that this new technology can also be used to perform coherent atom optics with BECs. Our storage ring will be highly adaptable, have a long (≈ 1 minute) trapping lifetime, and have good optical access (for both imaging and manipulation). In addition, as the BEC will be prepared within the ring, coherently transferring the atoms into the ring from a separate BEC creation site is not necessary.

A good atomic source can greatly lower the duration of BEC experiments. To this end we have realised an ^{87}Rb magneto-optical trap (MOT) [6] with a relatively large atom number ($N = 2 \times 10^9$). The MOT was formed using low powers (40 mW) of trapping light generated by a simple diode laser system [7]. The 780 nm $5s^2S_{1/2}, F = 2 \rightarrow 5p^2P_{3/2}, F = 3$ trapping light is red-detuned by 20 MHz and comprised of three retro-reflected two inch diameter laser beams. The loading rate of the MOT is controlled by the current passing through SAES alkali metal dispensers [8]. This MOT, situated in the high pressure end of the differentially-pumped XHV vacuum chamber of Fig. 1, will be used as a high-flux ($\approx 10^{10}$ atoms/s) source to multiply-load [9] a second ‘low pressure’ MOT in another chamber. We note that our atomic source should yield comparable performance to a Zeeman slower [10], without the added complexity.

The ‘low pressure’ MOT will be formed within a ‘square donut’ quartz vacuum cell (Fig. 2). This MOT will be an elongated [11], forced dark [12] MOT which should decrease light-assisted losses. The high product of the MOT loading rate and lifetime will yield a large trapped atom population. Ex-vacuo coils will be used for subsequent magnetic trapping of the atoms in a localised region of the toroidal magnetic trap illustrated in Fig. 3.

The currents of our magnetic coils (Fig. 3) will be regulated by five water-cooled MOSFET banks [13], and all currents will originate from the same 5 V, 500 A power supply, ensuring optimal magnetic field noise cancellation [14] when the coils are connected in series configurations. Our magnetic coil design allows us to realise many different magnetic geometries. Quadrupolar toroidal confinement will be provided by the circular coils (Fig. 3), which have mean diameters of 7.5 and 12.5 cm. Each coil carries a current of $2I_q = 0 - 2 \times 500$ A, yielding a maximum quadrupole magnetic field gradient of 227 G/cm. An azimuthal bias field can be added at the minimum of the toroidal field using the black straight wire, preventing spin-changing Majorana flops [15] in a purely toroidal trap. The rectangular ‘pinch’ coils in Fig. 3 localise atoms within the torus, and moreover they can be used in two distinct geometries, namely quadrupole and Ioffe-Pritchard (IP) [16] configurations. The two left rectangular coils are hard-wired in series, as are the right pair of coils. These left and right pinch coil pairs carry currents of $4I_l = 0 - 4 \times 500$ A (with $I_l \leq I_q$) and $4I_r = \pm 4I_l$ respectively. The geometry of the rectangular coils is such that if $I_l = I_r$, then in conjunction with the circular coils, an IP magnetic trap is formed. In contrast, if $I_l = -I_r$ then the rectangular coils are equivalent to anti-Helmholtz coils.

In the IP configuration the rectangular coils are designed to provide axial curvature to the trap (up to 55 G/cm²), whilst the axial bias field is minimised (≈ 0.9 G). Thus the optimal axial and radial magnetic trapping frequencies are 10 Hz and 305 Hz respectively – certainly adequate for condensate formation [17]. In the ‘anti-Helmholtz’ configuration the rectangular coils yield a maximum axial gradient of -67 G/cm (and the 227, -227 G/cm radial gradients from the toroidal quadrupole coils change to 207, -140 G/cm).

As the same coils are used for the MOT and the IP magnetic trap, the centres of the two magnetic fields overlap, and any possible ‘sloshing’ effects during transfers are eliminated. The adjustable nature of the axial magnetic field in both MOT and IP trap configurations also enables excellent mode-matching between the two traps.

*Electronic address: a.arnold@phys.strath.ac.uk; URL: <http://www.photonics.phys.strath.ac.uk/People/Aidan/Aidan.html>

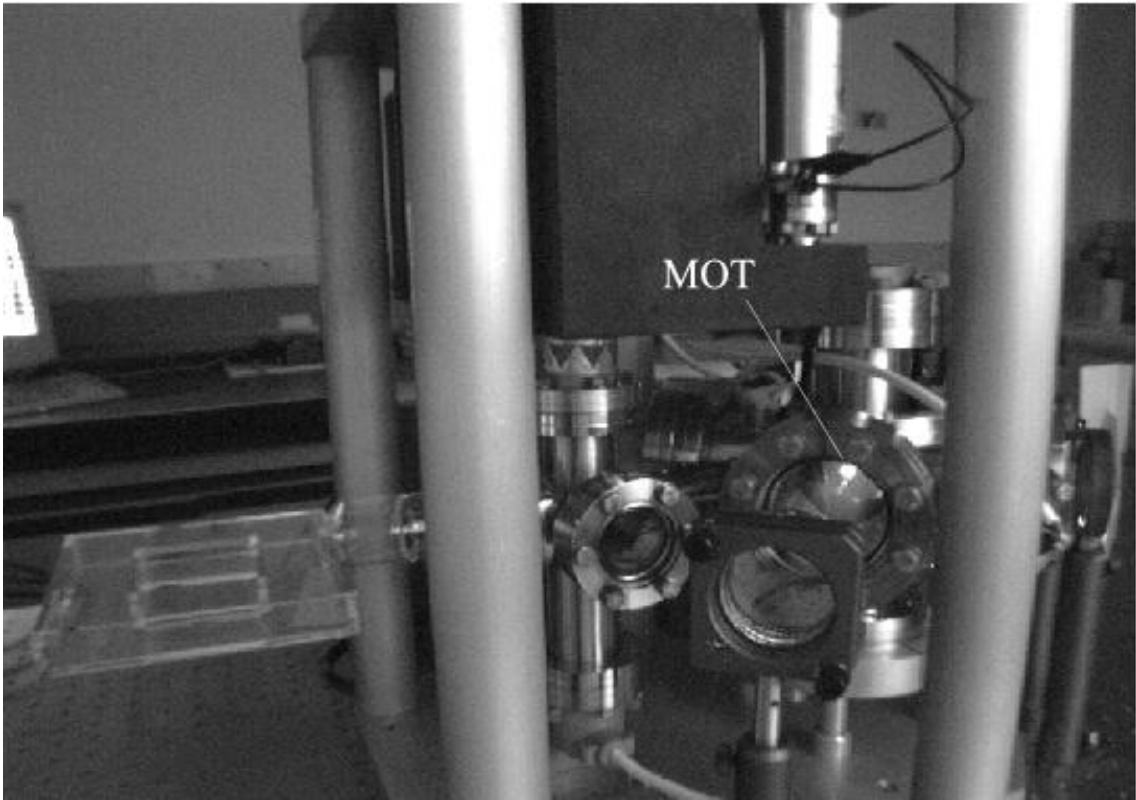


FIG. 1: The vacuum system consists of a ‘high pressure’ conflat cross (right) where an $N = 2 \times 10^9$ atom ^{87}Rb MOT is now formed. This MOT will be used to multiply load the special toroidal ‘low pressure’ quartz vacuum cell (enlarged in Fig. 2) which already yields pressures less than 4×10^{-11} torr.

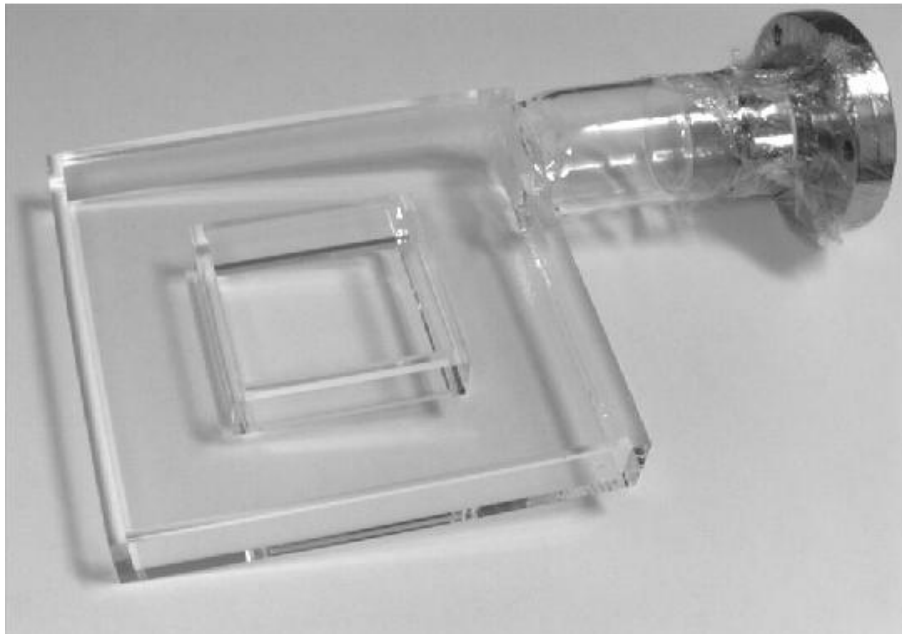


FIG. 2: The ‘square torus’ high optical quality quartz vacuum cell. The side-length of the square chamber is 12.5 cm.

The coils will initially be set to $I_q = I_l = -I_r = 36$ A, yielding radial and axial magnetic field gradients of

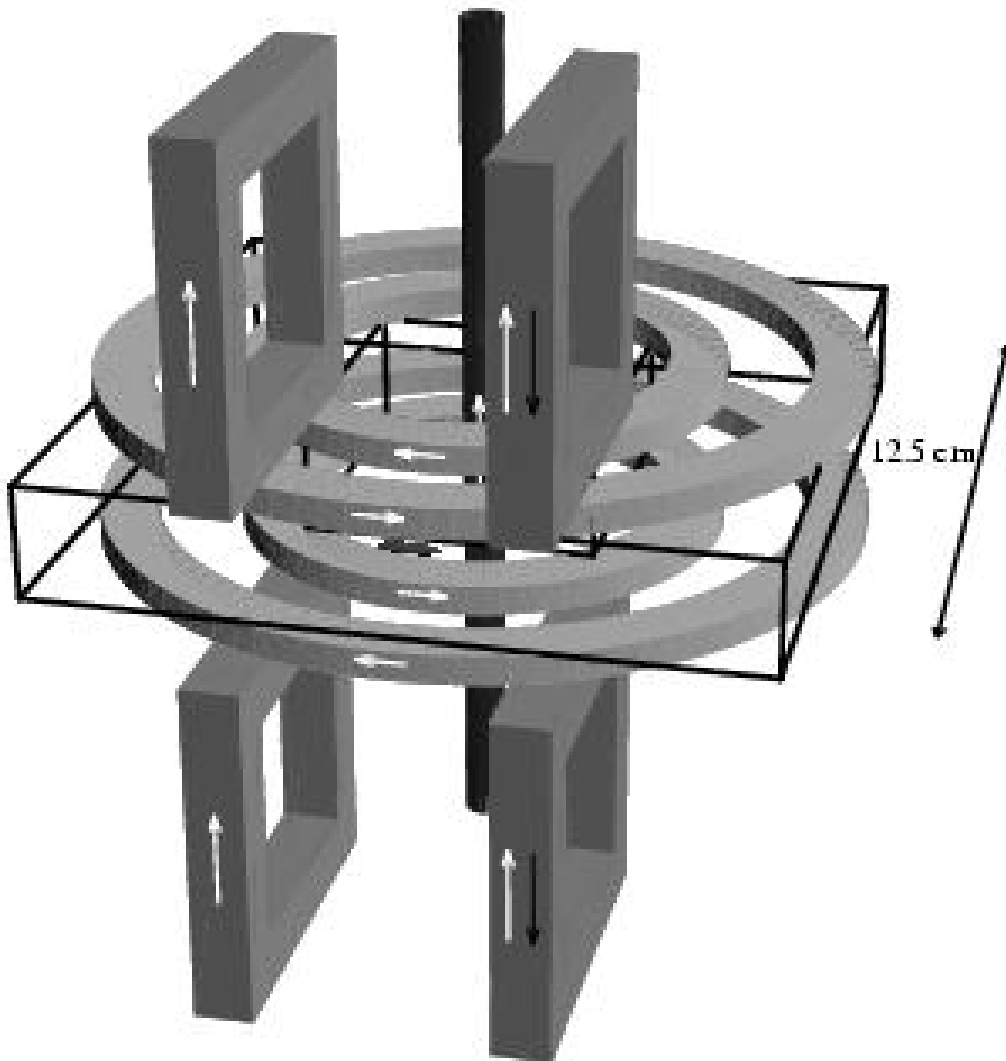


FIG. 3: The magnetic trap coils (to scale). Arrows indicate current directions in the various coils. The small elliptical cloud represents the axially elongated low pressure MOT/magnetic trap.

approximately = 15, -10 G/cm and -5 G/cm respectively. This provides an optimal field [18] for creating the ‘low pressure’ MOT. The aspect ratio of this MOT cloud will therefore be 0.7:1:1.2 (cf. 0.7:1:1 for a ‘standard’ MOT). Once this MOT contains a few 10^9 atoms, then the MOT can be elongated axially by reducing the current $I_l = -I_r$ in the rectangular coils. Atoms will not be collected directly in the elongated MOT due to its shallow axial depth and short lifetime.

The atoms in the elongated MOT will then be released into optical molasses for a few milliseconds, before being optically pumped into the $|F, m_F\rangle = |2, 2\rangle$ weak-field seeking state. Due to the elongated geometry of the MOT, we expect that the atoms at this stage should have a temperature as low as $10 \mu\text{K}$, and a peak density of a few 10^{11}cm^{-3} . By reversing the current I_r , the atoms will then be rapidly ($\ll 1$ ms) loaded into the IP-type magnetic trap ($I_q = I_l = I_r$) described above.

The magnetically trapped atoms can then be compressed by ramping up the current in the magnetic coils. This increases the inter-atomic elastic collision rate to facilitate efficient (‘runaway’) radio-frequency evaporation, which occurs when the ratio of elastic:inelastic collisions is above $\approx 200:1$ [13, 19]. The use of a ‘dark’ MOT will probably not

be necessary for reaching the runaway evaporation threshold [20], however it will increase the condensate population. If more magnetic compression is necessary, current can be passed through the vertical wire (Fig. 3), and the MOT can be loaded into an IP trap with an (initially) large bias field. After implementing a suitable evaporation trajectory, condensation will occur in the Ioffe-Pritchard trap in essentially the same manner as in most alkali BEC experiments to date.

By ramping down the current in the magnetic trap's pinch coils, atoms can subsequently access the entire torus, either by adiabatic expansion using the pinch coils followed by non-adiabatic expansion, or using a Bragg launching scheme. An important issue which needs to be addressed is the coherence of the condensate. It can be shown [20] that the coherence length of a non-interacting isotropic BEC is given simply by the width of the condensate. This result has also been seen experimentally along the 'short' dimension of a cigar-shaped interacting condensate [21]. One might therefore naively expect that both the physical and coherence lengths of an axially adiabatically expanding BEC would remain equal, especially as the 'phase-space density' of the condensate should remain well above one even if the condensate is released non-adiabatically into the storage ring. However, recently attention has been drawn to the issue of phase-fluctuations along the 'long' axis of cigar-shaped interacting BECs [22], and such phase-fluctuations have now been seen experimentally [23]. We also hope to study phase-fluctuations, however their presence makes interferometry somewhat difficult, and we will instead use a Bragg launching scheme (described below) to initiate toroidal BEC motion.

Second-order Bragg scattering [21, 24] will be used to (multiply) launch well-localised, *phase-coherent* atomic pulses (with very slowly decaying phase-space density) out of the BEC, very shortly after the pinch coils are turned off. One therefore avoids the large divergence of atomic orbits that occur if one simply releases the BEC at the top of a vertically oriented storage ring. The Bragg-scattered condensate pulses will be launched in both directions around the ring. Due to their initial velocity of 2.4 cm/s, one can only 'lift' the BEC packets $h = 30 \mu\text{m}$ vertically against gravity (or up a magnetic field 'hill' of 45 mG), and it is therefore important to form the BEC at the 'high' point of the toroidal potential. For this reason we will tilt the axis of the toroidal trap with respect to gravity, making the restrictions on magnetic field ripples less stringent. Even vertical orientations of the magnetic ring are possible, as it contains all atoms travelling at $< 1.6 \text{ m/s}$.

Our 'open' experimental geometry is well-suited to condensate investigation, in particular for imaging the atoms. The high degree of optical access will also facilitate the application of dipole force laser beams for manipulating the BEC in persistent current/Josephson effect experiments. The Sagnac rotational effect is proportional to the enclosed area of the beams in an interferometer. The single-revolution enclosed area of our toroidal trap is $\approx 140 \text{ cm}^2$, which is more than six hundred times the area of the state-of-the-art thermal atomic beam gyroscope [25]. Due to the long lifetime of our magnetic trap, we envisage that BEC pulses could rotate around the storage ring hundreds of times [5], further enhancing the interferometer's sensitivity. Additionally, it is hoped that the minimum detectable phase shift ($\delta\phi \approx 1/\sqrt{N}$) decreases to $\delta\phi \approx 1/N$ [26] when coherent atoms such as BECs are used, and higher precision Sagnac effect measurement should therefore be possible. The magnetic trap will also provide a good testing ground for investigations into the behaviour of one-dimensional quantum gases.

Acknowledgments: ASA is supported by a Royal Society of Edinburgh/Scottish Executive Education and Lifelong Learning Department research fellowship and the experiment is funded by the UK Engineering and Physical Sciences Research Council.

-
- [1] Anderson, M. H., *et al.*, 1995, *Science*, **269**, 198; Davis, K. B., *et al.*, 1995, *Phys. Rev. Lett.*, **75**, 3969; Bradley, C. C., *et al.*, 1995, *Phys. Rev. Lett.*, **75**, 1687.
 - [2] See for example the GSU BEC webpage: <http://amo.phy.gasou.edu/bec.html/>
 - [3] Ketterle, W., and Pritchard, D. E., 1992, *Appl. Phys. B*, **54**, 403.
 - [4] Cromptoets, F. M. H., *et al.*, 2001, *Nature*, **411**, 174.
 - [5] Sauer, J. A., Barrett, M. D., and Chapman, M. S., xxx.lanl.gov/abs/quant-physics/0108138.
 - [6] Raab, E. L., *et al.*, 1987, *Phys. Rev. Lett.*, **59**, 2631.
 - [7] Arnold, A. S., Wilson, J. S., and Boshier, M. G., 1998, *Rev. Sci. Instrum.*, **69**, 1236.
 - [8] Wieman, C., and Flowers, G., 1995, *Am. J. Phys.*, **63**, 317; Fortagh, J., *et al.*, 1998, *J. Appl. Phys.*, **84**, 6499; Rapol, U. D., *et al.*, 2001, *Phys. Rev A*, **64**, 023402.
 - [9] Gibble, K., Chang, S., and Legere, R., 1995, *Phys. Rev. Lett.*, **75**, 2666; Myatt, C. J., *et al.*, 1996, *Optics Lett.*, **21**, 290.
 - [10] Phillips, W. D., and Metcalf, H., 1982, *Phys. Rev. Lett.*, **48**, 596; Barrett, T. E., *et al.*, 1991, *Phys. Rev. Lett.*, **67**, 3483.
 - [11] Dudle, G., *et al.*, 1996, *J. Phys. B*, **29**, 4659.
 - [12] Ketterle, W., *et al.*, 1993, *Phys. Rev. Lett.*, **70**, 2253.
 - [13] Arnold, A. S., 1999, PhD thesis, University of Sussex.
 - [14] Mewes, M. O., *et al.*, 1997, *Phys. Rev. Lett.*, **78**, 582.

- [15] Petrich, W., *et al.*, 1995, *Phys. Rev. Lett.*, **74**, 3352.
- [16] Pritchard, D. E., 1983, *Phys. Rev. Lett.*, **51**, 1336.
- [17] Arnold, A. S., MacCormick, C., and Boshier, M. G., submitted to *Phys. Rev. Lett.*
- [18] Lindquist, K., Stephens, M., and Wieman, C., 1992, *Phys. Rev. A*, **46**, 4082.
- [19] Luiten, O. J., Reynolds, W. M., and Walraven, J. T. M., 1996, *Phys. Rev. A*, **53**, 381.
- [20] Arnold, A. S., and Boshier, M. G., to be published.
- [21] Stenger, J. *et al.*, 1999, *Phys. Rev. Lett.*, **82**, 4569.
- [22] Petrov, D. S., Shlyapnikov, G. V., and Walraven, J. T. M., 2001, *Phys. Rev. Lett.*, **87**, 050404.
- [23] Dettmer, S., *et al.*, xxx.lanl.gov/abs/cond-mat/0105525.
- [24] Kozuma, M., *et al.*, 1999, *Phys. Rev. Lett.*, **82**, 871.
- [25] Gustavson, T. L., *et al.*, 1997, *Phys. Rev. Lett.*, **78**, 2046.
- [26] Jacobson, J., Björk, G., and Yamamoto, Y., 1995, *Appl. Phys. B*, **60**, 187.

This figure "Fig1.jpg" is available in "jpg" format from:

<http://arxiv.org/ps/cond-mat/0110295v1>

This figure "Fig2.jpg" is available in "jpg" format from:

<http://arxiv.org/ps/cond-mat/0110295v1>

This figure "Fig3.jpg" is available in "jpg" format from:

<http://arxiv.org/ps/cond-mat/0110295v1>